Energy transport and optimal design of noisy Platonic quantum networks

C. Javaherian and C. Ferrie

Centre for Quantum Software and Information, University of Technology Sydney, Australia

August 2, 2022

Abstract

Optimal transport is one of the primary goals for designing efficient quantum networks. In this work, the maximum transport is investigated for three-dimensional quantum networks with Platonic geometries affected by dephasing and dissipative Markovian noise. The network and the environmental characteristics corresponding the optimal design are obtained and investigated for five Platonic networks with 4, 6, 8, 12, and 20 number of sites that one of the sites is connected to a sink site through a dissipative process. Such optimal designs could have various applications like switching and multiplexing in quantum circuits.

Introduction

Transport is an essential phenomena in atomic-scale devices and networks. The structure that hosts the energy or information carriers could be a continuous medium like metallic nanorods and waveguides [1, 2] or site-based structure like metallic nanoparticle arrays [3, 4], quantum dot arrays [5, 6], and many more. Discrete or site-based transport — considered in this work — has many applications such as quantum state transport through spin chains [7, 8, 9, 10], quantum energy transport in chains of trapped ions, environment-assisted transport in networks of sites [11, 12], and switching with qubit arrays [13]. While much is known for ideal networks, the effect of noise on the desired properties are less understood. We study the case of noisy quantum networks here. A specific type of quantum network that has been proven to have exact theoretical solutions for site-based energy excitation transfer are called Fully Connected Networks (FCNs) [14]. FCNs are defined by the property that all sites are equally connected to each other and the last site is dissipatively connected to a sink site. In [15] we studied some three dimensional Platonic configurations with distance dependent couplings, and proved that they have some similar properties as those of an N-site FCN, where in the corresponding Platonic network $N - 1$ would be the number of nearest neighbours of each site. For example, it was shown that the sink population — the energy excitation accumulated in the sink site — of the "noiseless" Platonic quantum networks and FCNs are the same at the steady state (or infinite time). These identities are convenient and powerful tools for the study quantum networks, and we find similar relations in the more relevant case of *noisy* quantum networks.

In this work we prove that in different noisy Platonic quantum networks the analytical solution of the steady sink population is the same as that of the equivalent FCN. In addition, we provide some relations among the couplings and noise rates corresponding to the maximum transport. These relations will be useful to optimally design such quantum networks for various applications such as transport through three dimensional Platonic networks, or switching and multiplexing in quantum circuits. The latter could be achieved by changing the environmental noise rates (electrical or magnetic) around the last site connected to the sink site, in a quantum dot or photonic qubits implementations, so that the incoming excitation would be transferred to the planned sink site.

Before presenting our results, we comment on two advantages of using Platonic quantum networks for such purposes. First, three dimensional networks in general are more compact in comparison

with two and one dimensional networks, and the nanoscale 3D printing methods [16, 17] could help to overcome the 3D construction difficulties. The three dimensional structures might also be compatible with the physics or other constraints of some architectures. The other advantage of Platonic quantum networks is that they are proven to be a FCN network with reduced number of sites that has exact transport solutions, and thus ideal benchmarks for new techniques and demonstrations.

Results

A Platonic network in this work is defined as a group of interactive identical two-level systems, located on the vertices of one of the five Platonic geometries, depicted in Fig.1, and one additional site (sink site) is irreversibly connected to one of the main sites with rate Γ. We assume a homogeneous environment so that all sites (main qubits) are affected by equal dissipation and dephasing Markovian local noises with rates Γ_{diss} and γ, respectively.

Figure 1: The schematic of the five Platonic geometries. Left to right: Tetrahedron (4 vertices), Cube (8 vertices), Octahedron (6 vertices), Icosahedron (12 vertices), and Dodecahedron (20 vertices)

.

The Hamiltonian (in units $\hbar = 1$) of the Platonic network would be

$$H = \sum_{i=1}^{N} J_{ij}\sigma_i^\dagger \sigma_j + c.c., \tag{1}$$

where N is the total number of main sites, J_{ij} is the distance-dependent coupling between qubits i, j, $\sigma_i^\dagger(\sigma_i)$ is the creation (annihilation) operator, and $c.c.$ denotes the complex conjugation of the fist part. The dynamics of the total density matrix of this system is found by a Lindbladian master equation [18] as follows:

$$\dot{\hat{\rho}} = -i[\hat{H}_{\mathrm{sys}}, \hat{\rho}] + \mathcal{L}_{\mathrm{target}}(\hat{\rho}) + \mathcal{L}_{deph}(\hat{\rho}) + \mathcal{L}_{\mathrm{diss}}(\hat{\rho});$$

$$\mathcal{L}_{\mathrm{target}}(\hat{\rho}) = \Gamma(2\hat{\sigma}_{\mathrm{target}}^\dagger \hat{\sigma_N}\hat{\rho}\hat{\sigma_N}^\dagger \hat{\sigma}_{\mathrm{target}} - \left\{\hat{\sigma_N}^\dagger \hat{\sigma}_{\mathrm{target}}\hat{\sigma}_{\mathrm{target}}^\dagger \hat{\sigma_N}, \hat{\rho}\right\}),$$

$$\mathcal{L}_{deph}(\hat{\rho}) = \gamma \sum_{i=1}^{N}(2\hat{\sigma}_i^\dagger \hat{\sigma}_i\hat{\rho}\hat{\sigma}_i^\dagger \hat{\sigma}_i - \left\{\hat{\sigma}_i^\dagger \hat{\sigma}_i, \rho\right\}),$$

$$\mathcal{L}_{\mathrm{diss}}(\hat{\rho}) = \Gamma_{\mathrm{diss}}(2\hat{\sigma}_{\mathrm{target}}^\dagger \hat{\sigma_N}\hat{\rho}\hat{\sigma_N}^\dagger \hat{\sigma}_{\mathrm{target}} - \left\{\hat{\sigma_N}^\dagger \hat{\sigma}_{\mathrm{target}}\hat{\sigma}_{\mathrm{target}}^\dagger \hat{\sigma_N}, \hat{\rho}\right\}), \tag{2}$$

where we assumed $\hat{\rho} = \hat{\rho}_{\mathrm{qubits}} \oplus \hat{\rho}_{\mathrm{target}} \oplus \hat{\rho}_{\mathrm{discharge}}$, is the direct sum of the $N \times N$ density matrix of the Platonic network ($\hat{\rho}_{\mathrm{qubits}}$), the 1×1 population matrix of the sink site ($\hat{\rho}_{\mathrm{target}}$), and the 1×1 matrix representing the total population discharged to the environment by dissipation noise ($\hat{\rho}_{\mathrm{discharged}}$). γ, and Γ_{diss} are the dephasing and dissipation noise rates to the environment from the network sites to the surrounding environment. Γ is the rate of irreversible energy transfer from the last site to the target site and $\hat{\sigma}_i^\dagger(\hat{\sigma}_i)$ is the creation (annihilation) operator of site i. We aim to provide an analytical expression for the population of target sink i.e. $\rho_{(N+1),(N+1)}(t) = \rho_{\mathrm{target}}(t)$ in the equilibrium state i.e. $t \to \infty$.

In order to simplify the analytical calculation, we study the dynamical characteristics of Platonic networks by numerically solving $\rho(t)$ from Eq.(2). For the simulation, the ion qubits implementation of the Platonic networks is assumed in which the coupling rate, or the interaction energy between two dipoles of ion qubits i and j would be inversely proportional to the cube of their interconnecting distance ($J_{ij} = v/r_{ij}^3$, $v = 1$). In Figs.2,3,4 we plotted the sites' populations ($\rho_{ii}(t)$) of four Platonic networks in the noiseless case ($\gamma = \Gamma_{diss} = 0$). It can be seen that the populations of some sites vary inversely in some cases, while other sites would have same population dynamics.
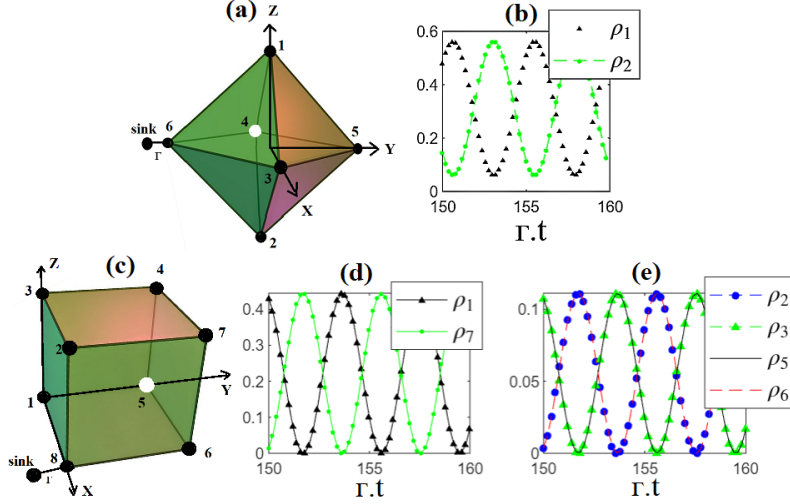
Figure 2: This graph shows the simulated population dynamics of all sites ($\rho_{ii} \equiv \rho_i$, $i = 1...N = 6, 8$) of tetrahedron and cube noiseless networks with zero environmental noises ($\gamma = \Gamma_{diss} = 0$), where the sink site ($i = N + 1$) is dissipatively connected to the Nth site with rate Γ. Parts (a) and (b) show the schematics of the tetrahedron and cube networks with 6 and 8 sites on the vertices. The sites coordinates for tetrahedron are $(0, 0, \pm\frac{1}{\sqrt{2}}), (0, \pm\frac{1}{\sqrt{2}}, 0), (\pm\frac{1}{\sqrt{2}}, 0, 0)$, and for the cube (graph (c)), site 1 is located at the origin of coordinates and its symmetrically positioned site (7) is located at $(1, 1, 1)$. In both networks, at $t = 0$, site No. 1 was charged by one excitation. Part (b) presents the oscillating populations of sites 1 and 2 in time that are positioned symmetrically with respect to the centre of the tetrahedron. Note that since the rate Γ has dimension $1/T$, the quantity $\Gamma.t$ is dimensionless. The population of the spherically symmetric sites (3,4) at equilibrium i.e. $\Gamma.t \gtrsim 20$ is constant (0.0625). The symmetrically positioned sites 5 and 6 are discharged at equilibrium while the sink site 7 is saturated to the population of 0.25. The graphs (d) and (e) show that the spherically symmetric sites (positioned symmetrically with respect to the centre of the cube), i.e. (1,7), (2,5) and (3,6) are oscillating inversely at equilibrium i.e. $\Gamma.t \gtrsim 20$. At equilibrium, the populations of the spherically symmetric sites 4 and 8 are zero since the population of the sink site (9) is saturated to 0.33.

The characteristics shown in these figures (noiseless cases) would be the same as that of noisy cases unless the fact that in the presents of dephasing and/or dissipation noises, the oscillating patterns of populations would be evanescent and the sink site would be fully populated at the equilibrium ($t \to \infty$). In [15] we found that the target population of noiseless Platonic networks at steady state are independent of their size and is only related to the number of neighboring sites ($N_c - 1$) as of $\rho_{sink} = 1/(N_c - 1)$, i.e. $\rho_{sink} = 0.25, 0.33, 0.2, 0.33$ for $N = 6, 8, 12, 20$, respectively. Later on, we conclude that the exact solution of the dynamics of Platonic networks are the same as that of FCNs, in which all sites are equidistant from each other [14]. Since the tetrahedron Platonic network (N=4) is a FCN by definition, we ignored its simulation since we do not need anymore to prove that its analytical solution of target population is as that of an FCN.

Figs.2 show the dynamics of two Platonic networks with N=6 and 8. It can be seen that some pair of sites are oscillating inversely, while the populations of other pairs of sites vary equally. To simplify the analytical solution, we will assume that the average of sites' populations (and the coherences) of these pairs could be assumed for one of the sites, and we would only solve the dynamics of a Platonic network for N_c sites. Figs.3 and 4 show the dynamics of Platonic networks with N=12 and N=20 sites, respectively. The graphs show that in these types of networks, for the chosen initial charges of each case, the populations of different groups of sites vary similarly. So likewise the other Platonic geometries, we simplify the analytical dynamics by assuming only a specific number of sites i.e. N_c sites. So if $\rho(t)$ would be the density matrix of a platonic network of N sites, with rank $(N + 2)$ and elements $\rho_{ij}(t)$, we define the following symbolic density matrix $\tilde{\rho}(t)$ of an equivalent network of N_c sites, with rank $(N_c + 2)$ and symbolic elements of $\tilde{\rho}_{ij}(t)$ defined as follows. Note that in the legends of Figs. 2,3,4 and the two following formulas, we consider the notation $\rho_{ii}(t) \equiv \rho_i(t)$ for simplicity.
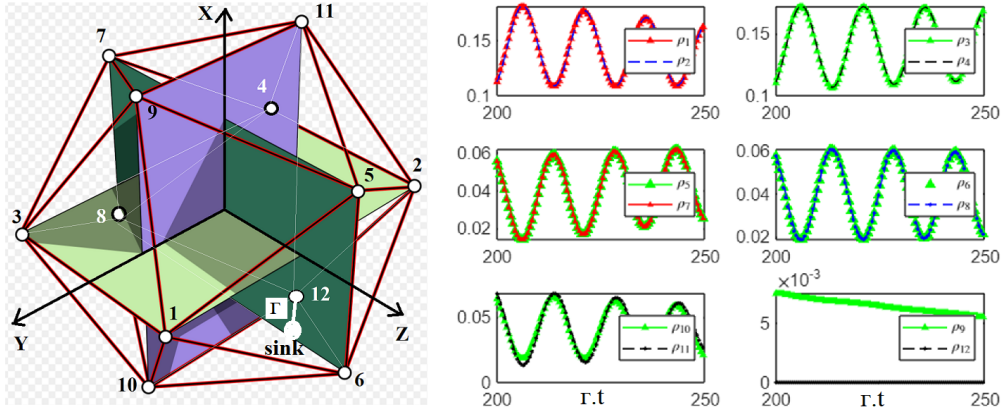
3

Figure 3: This graph shows the simulated population dynamics of all sites ($\rho_{ii} \equiv \rho_i$, $i = 1...N = 12$) of a regular icosahedron noiseless network with zero environmental noises ($\gamma = \Gamma_{diss} = 0$), where the sink site ($i = N + 1 = 13$) is dissipatively connected to only one site (12) with rate Γ. The left graph shows the schematic of the icosahedron network where sites are located on the vertices with coordinates $(0, \pm\phi, \pm 1), (\pm 1, 0, \pm\phi), (\pm\phi, \pm 1, 0)$ where $\phi = (1 + \sqrt{(5)})/2$. At $t = 0$ four sites (1,2,3,4) are equally charged by $1/4$ amount of excitation. The right graphs show that due to the various symmetries in Platonic geometries, some sites are oscillating similarly (sites "1,2", "3,4", "5,7", "6,8", and "10,11"), at the equilibrium i.e. $\Gamma.t \gtrsim 20$. In addition, the populations of the spherical-symmetrically positioned sites of 12 and 9, are zero, since the population of the sink site (13) is saturated to 0.2 at equilibrium.

$$N = 6:$$
$$\tilde{\rho}_1(t) = \rho_1(t) + \rho_2(t),$$
$$\tilde{\rho}_i(t) = \rho_i(t), \ i \neq 1, 2$$
$$N = 8, 12:$$
$$\tilde{\rho}_i(t) = \rho_i(t) + \rho_{\tilde{i}}(t),$$
(3)

where $\tilde{i}$ is the index of the spherical-symmetrically positioned site with respect to site i. So the number of symbolic sites of $N = 6$ network is $N_c = 5$, and that of $N = 8$ and 12 are $N_c = 4$ and $N_c = 6$, respectively. For $N = 20$, according to Fig.4 we choose:

$$N = 20:$$
$$\tilde{\rho}_1(t) = \rho_1(t) + \rho_5(t) + \rho_9(t) + \rho_{20}(t),$$
$$\tilde{\rho}_2(t) = \rho_2(t) + \rho_6(t) + \rho_{10}(t) + \rho_{19}(t),$$
$$\tilde{\rho}_3(t) = \rho_3(t) + \rho_8(t) + \rho_{12}(t) + \rho_{13}(t) + \rho_{16}(t) + \rho_{17}(t),$$
$$\tilde{\rho}_4(t) = \rho_4(t) + \rho_7(t) + \rho_{11}(t) + \rho_{14}(t) + \rho_{15}(t) + \rho_{18}(t),$$
(4)

So the number of symbolic sites of $N = 20$ network is $N_c = 4$, The above two formulas show that we assume $N_c = 5, 4, 6, 4$ symbolic sites, for five Platonic networks with $N = 6, 8, 12, 20$ sites. Note that the distance between the chosen group of sites, assumed as one symbolic site, with the other neighboring group of sites are all equal. Now the coherences between the sites of the equivalent reduced networks would be defined according to the symbolic indices as

$$\tilde{\rho}_{ij}(t) = \sum_{p=1}^{n} \sum_{q=1}^{m} \rho_{pq}(t),$$
(5)

where n, m are the number of sites that define the symbolic sites i, j, respectively, that is $\tilde{\rho}_{ii}(t) \equiv \tilde{\rho}_i(t) = \sum_{p=1}^{n} \rho_p(t)$ and $\tilde{\rho}_{jj}(t) \equiv \tilde{\rho}_j(t) = \sum_{q=1}^{n} \rho_q(t)$. As an example, in a dodecahedron network:

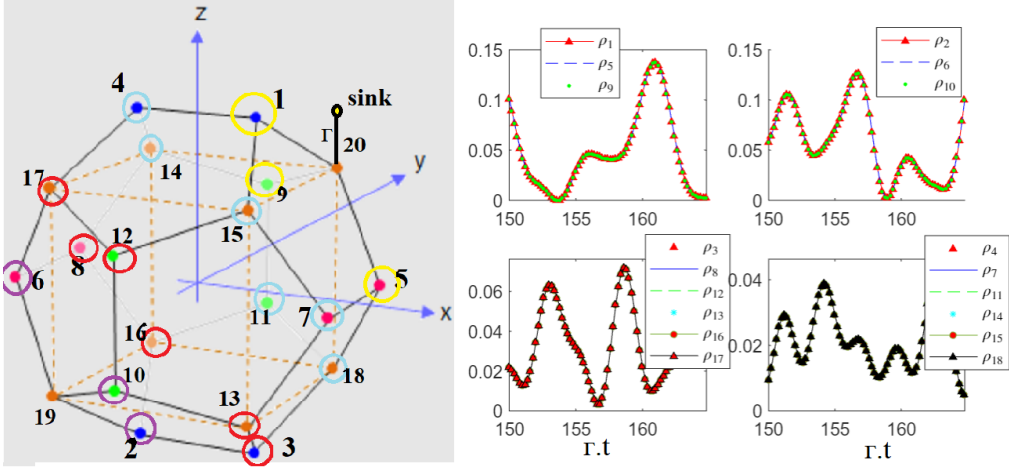$$\tilde{\rho}_{12}(t) = \sum_{\substack{p=\{1,5,9,20\}, \\ q=\{2,6,10,19\}}} \rho_{pq}(t).$$
(6)

4

Figure 4: This graph shows the simulated population dynamics of all sites ($\rho_{ii} \equiv \rho_i, i = 1...N = 20$) of a regular dodecahedron noiseless network with zero environmental noises ($\gamma = \Gamma_{diss} = 0$), where the sink site ($i = N + 1 = 21$) is dissipatively connected to only one site (20) with rate Γ. The left graph shows the schematic of the icosahedron network where sites are located on the vertices with coordinates $(\pm 1, \pm 1, \pm 1), (0, \pm\phi, \pm\frac{1}{\phi}), (\pm\phi, 0, \pm\frac{1}{\phi}), (\pm\phi, \pm\frac{1}{\phi}, 0)$, where $\phi = (1 + \sqrt{(5)})/2$. At $t = 0$ three sites (1,5,9) are equally charged by 1/4 amount of excitation. The right graphs show that due to the various symmetries in Platonic geometries, some sites are oscillating similarly (sites "1,2", "3,4", "5,6,7,8", and "10,11"), at the equilibrium i.e. $\Gamma.t \gtrsim 20$. In addition, the populations of the spherically symmetric sites 19 and 20 are zero since the population of the sink site (21) is saturated to 0.33. There are four groups of sites on the right-side schematics that are marked with four different colors (violet, red, light blue, and yellow), that each group of sites posses similar populations. Adding two sites to red and yellow groups (sites No. 19 and 20, respectively), we create the four symbolic sites of the equivalent FCN of dodecahedron, as introduced in Eq.(4)

In future, for simplicity of notation, we substitute $\tilde{\rho}(t) \rightarrow \rho(t)$. Using the assumption of reduced networks, Eq.(2) would be written as follows:

$$
\begin{aligned}
\dot{\rho}_{ii} &= -2\Gamma_{\text{diss}}\rho_{ii} + iJ(R_i - \bar{R}_i); \ i \neq N, \\
\dot{\rho}_{ij} &= -2(\Gamma_{\text{diss}} + \gamma)\rho_{ij} + iJ(R_i - \bar{R}_j); \ (i,j) \neq N, \\
\dot{\rho}_{iN} &= -(2\Gamma_{\text{diss}} + 2\gamma + \Gamma)\rho_{iN} + iJ(R_i - \bar{R}_N), \\
\dot{\rho}_{\text{NN}} &= -(2\Gamma_{\text{diss}} + 2\gamma + \Gamma)\rho_{\text{NN}} + iJ(R_N - \bar{R}_N), \\
\dot{\rho}_{00} &= 2\Gamma_{\text{diss}}Tr_{N_c}(\rho), \\
\dot{\rho}_{\text{target}} &= 2\Gamma\rho_{\text{NN}},
\end{aligned}
\tag{7}
$$

where ρ_{00} correspond to a virtual site that stores a fraction of initial excitation within the environment through dissipative noise with rate Γ_{diss}, and the population of the last site ρ_{NN}, is being discharged dissipatively by rate Γ to the target site with corresponding matrix element $\rho_{(N+1),(N+1)}$. We assume the following collective variables:

$$
R_i(t) = \sum_{j=f_{N_c}(i)} \rho_{ij}(t), \ \Lambda_i = \sum_{j=f_{N_c}(i)} R_j,
\tag{8}
$$

where $f_{N_c}(i)$ is the set of N_c indices of the nearest neighbors of site i plus itself. The equations of motion of the collective variables would be as following:

$$
\begin{aligned}
\dot{R}_i &= -iJ\Lambda_i + iN_c J R_i - 2(\Gamma_{\text{diss}} + \gamma)R_i - \Gamma\rho_{iN} + 2\gamma\rho_{ii,} \\
\dot{R}_N &= -iJ\Lambda_N + iN_c J R_N - (2\Gamma_{\text{diss}} + 2\gamma + \Gamma)R_N + (2\gamma - \Gamma)\rho_{\text{NN}}, \\
\dot{\Lambda}_i &= -(2\Gamma_{diss} + \gamma)\Lambda_i + \Gamma(R_N + \bar{R}_N) + 2\gamma Tr_{N_c(i)}(\rho),
\end{aligned}
\tag{9}
$$

where

$$
Tr_{N_c(i)}(\rho) = \sum_{i=f_{N_c}(i)} \rho_{ii} = Tr(\rho).
\tag{10}
$$

5

Now from the rule of conservation of population we have:

$$1 = Tr(\rho) + \rho_{00} + \rho_{\text{target}}. \tag{11}$$

It indicates that the initial population would oscillate among all network sites, and partially accumulated in the surrounding environment and the target site, through the dissipation noise rates of $\Gamma_{\text{diss}}, \gamma$ and Γ, respectively.

Considering $R_N = x + iy$, Eq.(9) line 2 yields two first order differential equations for x and y which besides Eqs.(7) lines 4-6, Eq.(9) line 3 and Eq.(11), form a close set of differential equations for variables $x, y, \Lambda_N, \rho_{\text{NN}}, \rho_{00}, \rho_{\text{target}}$ as follows:

$$
\begin{aligned}
\dot{\Lambda}_N &= -2(\Gamma_{diss} + \gamma)\Lambda_N - 2\Gamma x + 2\gamma(1 - \rho_{00} - \rho_{\text{target}}), \\
\dot{x} &= -(2\Gamma_{diss} + 2\gamma + \Gamma)x + (2\gamma - \Gamma)\rho_{\text{NN}} - JN_c y, \\
\dot{y} &= -(2\Gamma_{diss} + 2\gamma + \Gamma)y + JN_c x - J\Lambda_N, \\
\dot{\rho}_{\text{NN}} &= -2(\Gamma_{diss} + \Gamma)\rho_{\text{NN}} - 2Jy, \\
\dot{\rho}_{00} &= 2\Gamma_{diss}(1 - \rho_{00} - \rho_{\text{target}}), \\
\dot{\rho}_{\text{target}} &= 2\Gamma\rho_{\text{NN}}.
\end{aligned}
\tag{12}
$$

According to Eq.(3) and Figs.2,3,4, the initial conditions for different Platonic networks are assumed as:

$$
\begin{aligned}
N = 6, 8 &: \\
&\rho_1(0) \equiv \rho_{11}(0) = 1, \ \rho_{ij}(0) = 0, i, j \neq 1 \\
N = 12 &: \\
&\rho_1(0) = \rho_2(0) = \rho_3(0) = \rho_4(0) = 1/4, \ \rho_{ij}(0) = 0, \ i \neq j \neq 1, 2, 3, 4 \\
N = 20 &: \\
&\rho_1(0) = \rho_5(0) = \rho_9(0) = 1/3, \ \rho_{ij}(0) = 0, \ i \neq j \neq 1, 5, 9
\end{aligned}
\tag{13}
$$

The above initial conditions yield:

$$
\begin{aligned}
R_N(0) &= \sum_{i \in f_{N_c}(N)} \rho_{Ni} = 0, \ x(0) = y(0) = 0, \\
\Lambda_N(0) &= \sum_{i \in f_{N_c}(N)} R_i(0) = R_N(0) + R_{i \neq \{1-4, N\} \text{ or}, i \neq \{1, 5, 9, N\}}(0) = 1.
\end{aligned}
\tag{14}
$$

Now by applying the Laplace transform to Eqs.(12) i.e. $t \to 1/s$, $\dot{\alpha}(t) \to \left(\tilde{\alpha}.s - \alpha(0)\right)$, we obtain:

$$
\begin{aligned}
(s + 2\Gamma_{diss} + 2\gamma)\tilde{\Lambda}_N + 2\Gamma\tilde{x} + 2\gamma\rho_{\text{target}} + 2\gamma\rho_{00} - 2\gamma/s - 1 &= 0, \\
(s + 2\Gamma_{diss} + 2\gamma + \Gamma)\tilde{x} + (\Gamma - 2\gamma)\tilde{\rho}_{\text{NN}} + JN_c\tilde{y} &= 0, \\
(s + 2\Gamma_{diss} + 2\gamma + \Gamma)\tilde{y} + J\tilde{\Lambda}_N - JN_c\tilde{x} &= 0, \\
(s + 2\Gamma_{diss} + 2\Gamma)\tilde{\rho}_{\text{NN}} + 2J\tilde{y} &= 0, \\
(s + 2\Gamma_{diss})\tilde{\rho}_{00} + 2\Gamma_{diss}\tilde{\rho}_{\text{target}} - 2\Gamma_{diss}/s &= 0, \\
s\tilde{\rho}_{\text{target}} - 2\Gamma\tilde{\rho}_{\text{NN}} &= 0.
\end{aligned}
\tag{15}
$$

Solving the complete set of Eqs.(15), the target sink population will be found for Platonic networks in the presence of homogeneous local noises as following:

$$
\begin{aligned}
\bar{\rho}_{\text{target}} &= 4\Gamma J^2 \frac{(\Gamma_B + s)(s + \Gamma_A)}{s\Delta(s)} \\
\Delta(s) &= 8\Gamma J^2\gamma(\Gamma_B + s) + (s + 2\Gamma_{\text{diss}}) \\
&\quad ((\Gamma_A + s)(\Gamma_C + s)(\Gamma_B + s)^2 \\
&\quad -4\Gamma J^2(\Gamma - 2\gamma) \\
&\quad -2J^2 N_c(\Gamma_A + s)(\Gamma - 2\gamma) \\
&\quad +2\Gamma J^2 N_c(\Gamma_C + s) \\
&\quad +J^2 N_c^2(\Gamma_A + s)(\Gamma_C + s)).
\end{aligned}
\tag{16}
$$

where

$$\begin{aligned}
\Gamma_A &= 2\gamma + 2\Gamma_{\mathrm{diss}}, \\
\Gamma_B &= 2\gamma + 2\Gamma_{\mathrm{diss}} + \Gamma, \\
\Gamma_C &= 2\Gamma_{\mathrm{diss}} + 2\Gamma
\end{aligned} \tag{17}$$

This expression is equivalent to that of an FCN network, i.e. Eqs.(A25, A26) of [14], where the Platonic coordinate number (N_c) is equivalent to the total number of sites. Since the root of the denominator in Eq.(16) does not have an analytical solution, the final target population of the considered Platonic networks are as following:

$$\rho_{\mathrm{target}}(t \to \infty) = \lim_{s \to 0}[s\bar{\rho}_{\mathrm{target}}] = 4\Gamma J^2 \frac{\Gamma_B \Gamma_A}{\Delta(0)} \tag{18}$$

It can be seen that in the noiseless environment ($\gamma, \Gamma \to 0$), the steady state target population is the same as the previous expression found in [15] i.e. $1/(N_c - 1)$, which can be here achieved by first tending the local dephasing rate to zero. If first tending the local dissipation rate to zero, the target population tends to 1. This is due to the fact that the local dissipation noise would only discharge the excitation from each site to the environment and not to the other sites, however the dephasing noise provides new paths of energy transport within network sites, leading to discharge of all excitation to the target site through the Nth site.
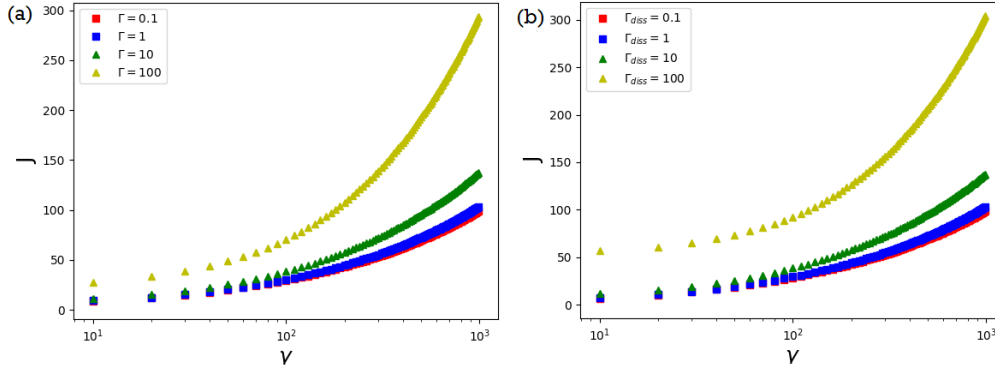

Figure 5: The relation of network and environment variables in a noisy cubic Platonic network with optimal transport to the target site at steady state. Graph (a) shows the relation of coupling rate J and dephasing noise γ for different amounts of dissipation rate to the sink (Γ), while dissipation rate to the local environments are fixed at $\Gamma_{\mathrm{diss}} = 10$. Graph (b) shows the same relations for different values of Γ_{diss} and fixed amount of $\Gamma = 10$. It could be indicated from the graphs that the coupling strength should be increases by increasing other parameters to maintain the full transport. The values of parameters could be used for optimal design of Platonic networks.

From the numerical investigations we know that the maximum value of the target population in the presence of noises is one. To find the network-environment parameters corresponding the maximum excitation transport, we equate the target population of Eq.(18) to one, and find a relation among all network and environment parameters. The resulting equation can be used to find the optimal design variables. For example, the coupling rate J could be found in terms of other parameters. Figs.5(a),(b) show the relation between J, the coupling rate between the nearest neighbors in Platonic networks, and the Markovian dephasing rate γ, for different values of dissipation rates from each site to the environment (Γ_{diss}), and also the different values of dissipation rates from the Nth site to the sink site (Γ). The network of consideration for both parts (a) and (b) is a cubic lattice with $N = 8$ main sites, and the constant parameters are $\Gamma_{\mathrm{diss}} = 10$ and $\Gamma = 10$, respectively. It can be seen in Fig.5 that for the fixed chosen parameters, by increasing the dephasing rate, the coupling strength should be increased, so that the disturbing effect of dephasing noise would be compensated on energy transport towards the sink.

It can be also seen from Fig.5(a) that for a fixed depahsing noise rate γ and the fixed chosen dissipation noise rate $\Gamma_{\mathrm{diss}} = 10$, to maintain the maximum transport, the nearest neighbors
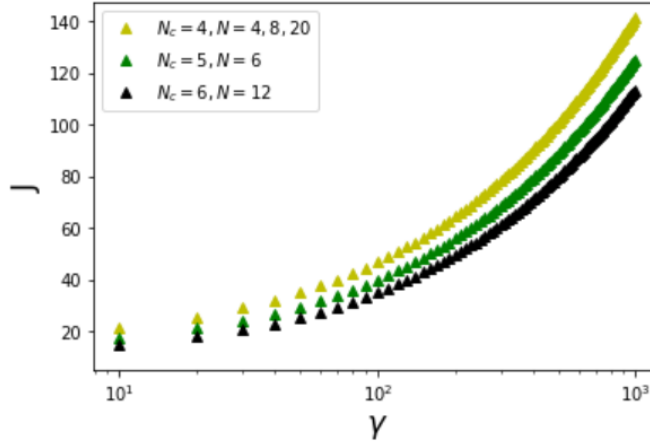
Figure 6: This graph shows the relation of sites' couplings and the environmental dephasing rate for different Platonic networks with optimal transport at steady state. It could be seen that for networks with more Nc or number of nearest neighbours, the coupling rate J of each pair of sites is less. This indicates that more sites with less coupling strength are equivalent to less number of sites with higher coupling rates.

sites couplings should be increased, by increasing the dissipation rate to the target sink (Γ). In other words, in the fixed environment with the same dephasing and dissipation noise rates, the higher sites' couplings demands faster noise rates to the sink site to obtain the optimal design corresponding the maximum energy transfer. To understand this behaviour, note that the higher sites' coupling rate results in stronger and more energy bouncing among the sites, that demands higher coupling rate towards the sink. It should be also taken into account that the relation among the parameters for the maximum transport is nonlinear.

In such Platonic noisy networks, Since the nonzero dissipation rate of $\Gamma_{\mathrm{diss}} = 10$ will irreversibly transfer some energy to the environment, to reach the full energy transport, the coupling rate and the sink dissipation rate should be high or fast enough to transfer all energy before any fraction of that would be dissipated towards the surrounding environment. Part of this process could be supported by dephasing-noise-assisted-transport [11, 12]. This fact can be seen in Fig.5(b). It shows the relation of network-environment parameters for the fixed amount of $\Gamma = 10$. It can be seen that for a strong dissipation rate ($\Gamma_{\mathrm{diss}} = 100$), the sites' coupling rate should be increased to be able to transfer the energy fast enough before getting dissipated to the environment.

Fig.6 shows the optimal design graphs of Platonic networks with different number of sites. The constant parameters are chosen as $\Gamma_{\mathrm{diss}} = \Gamma = 10$. It can be seen that for a fixed dephasing rate, by increasing Nc of a Platonic network (the number of nearest neighbours of any site plus one), the coupling rate J should be decreased to obtain maximum transport. This could be understood by the fact that by increasing N_c, the number of interactions by a single site will be increased. So for given fixed initial excitation (one unit) to each Platonic network, we need less coupling rate between each pair of sites, to maintain maximum transport. In summary, Figs.5 and 6 provide information to design 3D noisy Platonic networks that can fully transfer the energy from the designated sites towards a target sink. Using these optimal design graphs help us to prevent the loss of energy excitation into the surrounding Markovian environment through local dissipation and dephasing noise rates.

Conclusion

Energy transport is an inevitable phenomenon in many atomic-scale networks. In this work, we numerically studied the characteristics of energy dynamics in Platonic quantum networks consists of $4, 6, 8, 12$, and 20 qubits, located on vertices of high symmetric 3D Platonic geometries. A target site was assumed to be dissipatively connected to one of the qubits. Due to the opposite or same patterns of populations' oscillations of qubits, we made an assumption of reducing the number of qubits of each network to an effective value which was equal to the number of one group of nearest neighbor sites within each network. We found the analytical expression for the target

site population in the presence of environmental Markovian dephasing and dissipation noises. In addition, we investigated the optimal design characteristics of Platonic network for maximum energy transport from the first site towards the target site. We plotted the relation between the coupling strength and the dephasing noise rate corresponding the maximum transport. The optimal designs of Platonic quantum networks could have several applications like switches or multiplexers in quantum devices. In the future, we hope to further analyse energy transport in three dimensional Platonic devices and investigate their physical implementations.

References

[1] Clara Javaherian and Babak Shokri. Guided dispersion characteristics of metallic single-wall carbon nanotubes. *Journal of Physics D: Applied Physics*, 42(5):055307, feb 2009.

[2] Clara Javaherian Yadollah Ahmadizadeh and Babak Shokri. Study of geometrical effects on the characteristics of metallic double-walled carbon nanotube waveguides through quantum hydrodynamics. *Physics of Plasmas*, 16:063501, April 2009.

[3] Chuanping Li, David Cahen, Ping Wang, Haijuan Li, Jie Zhang, and Yongdong Jin. Plasmonics yields efficient electron transport via assembly of shell-insulated au nanoparticles. *iScience*, 8:213 – 221, 2018.

[4] Stefan A. Maier, Pieter G. Kik, Luke A. Sweatlock, Harry A. Atwater, J. J. Penninkhof, A. Polman, Sheffer Meltzer, Elad Harel, Ari A.G. Requicha, Bruce E. Koel, and et al. Energy transport in metal nanoparticle plasmon waveguides. *MRS Proceedings*, 777:T7.1, 2003.

[5] F. R. Braakman, P. Barthelemy, C. Reichl, W. Wegscheider, and L. M. K. Vandersypen. Long-distance coherent coupling in a quantum dot array. *Nature Nanotech*, 8:432, 2013.

[6] Yun Ran Wang, Im Sik Han, Chao-Yuan Jin, and Mark Hopkinson. Precise Arrays of Epitaxial Quantum Dots Nucleated by In Situ Laser Interference for Quantum Information Technology Applications. *ACS Appl. Nano Mater.*, 3(5):4739, 2020.

[7] Matthias Christandl, Nilanjana Datta, Artur Ekert, and Andrew J. Landahl. Perfect state transfer in quantum spin networks. *Phys. Rev. Lett.*, 92:187902, May 2004.

[8] M. S. Tame, M. Paternostro, M. S. Kim, and V. Vedral. Quantum-information processing with noisy cluster states. *Phys. Rev. A*, 72:012319, Jul 2005.

[9] Tobias J. Osborne and Noah Linden. Propagation of quantum information through a spin system. *Phys. Rev. A*, 69:052315, May 2004.

[10] Daniel Burgarth and Sougato Bose. Conclusive and arbitrarily perfect quantum-state transfer using parallel spin-chain channels. *Phys. Rev. A*, 71:052315, May 2005.

[11] Clara Javaherian and Jason Twamley. Robustness of optimal transport in one-dimensional particle quantum networks. *Phys. Rev. A*, 90:042313, Oct 2014.

[12] Filippo Caruso, Nicolò Spagnolo, Chiara Vitelli, Fabio Sciarrino, and Martin B. Plenio. Simulation of noise-assisted transport via optical cavity networks. *Phys. Rev. A*, 83:013811, Jan 2011.

[13] Long Tian. Circuit qed and sudden phase switching in a superconducting qubit array. *Phys. Rev. Lett.*, 105:167001, Oct 2010.

[14] Filippo Caruso, Alex W. Chin, Animesh Datta, Susana F. Huelga, and Martin B. Plenio. Highly efficient energy excitation transfer in light-harvesting complexes: The fundamental role of noise-assisted transport. *J. Chem. Phys.*, 131:105106, August 2009.

[15] Clara Javaherian and Jason Twamley. Platonic quantum networks as coherence-assisted switches in perfect and imperfect situations. *Journal of Physics D: Applied Physics*, 48(23):235104, may 2015.

[16] Julian Hengsteler, Barnik Mandal, Cathelijn van Nisselroy, Genevieve P. S. Lau, Tilman Schlotter, Tomaso Zambelli, and Dmitry Momotenko. Bringing electrochemical three-dimensional printing to the nanoscale. *Nano Letters*, 21(21):9093–9101, 2021. PMID: 34699726.

[17] Tien-Jen Chang, Lukas Vaut, Martin Voss, Oleksii Ilchenko, Line Hagner Nielsen, Anja Boisen, , and En-Te Hwu. Micro and nanoscale 3d printing using optical pickup unit from a gaming console. *Commun Phys*, 4(23), 2021.

[18] Heinz-Peter Breuer and Francesco Petruccione. *The theory of open quantum systems*. Oxford University Press, 2007.